Cogn Neurodyn (2007) 1:225–235
DOI 10.1007/s11571-007-9017-x

RESEARCH ARTICLE

Modulation of synchrony without changes in firing rates

Jakob Heinzle · Peter König · Rodrigo F. Salazar

Received: 14 June 2006 / Accepted: 15 February 2007 / Published online: 14 July 2007

Abstract It was often reported and suggested that the synchronization of spikes can occur without changes in the firing rate. However, few theoretical studies have tested its mechanistic validity. In the present study, we investigate whether changes in synaptic weights can induce an independent modulation of synchrony while the firing rate remains constant. We study this question at the level of both single neurons and neuronal populations using network simulations of conductance based integrate-and-fire neurons. The network consists of a single layer that includes local excitatory and inhibitory recurrent connections, as well as long-range excitatory projections targeting both classes of neurons. Each neuron in the network receives external input consisting of uncorrelated Poisson spike trains. We find that increasing this external input leads to a linear increase of activity in the network, as well as an increase in the peak frequency of oscillation. In contrast, balanced changes of the synaptic weight of excitatory long-range projections for both classes of postsynaptic neurons modulate the degree of synchronization without altering the firing rate. These results demonstrate that, in a simple network, synchronization and firing rate can be modulated independently, and thus, may be used as independent coding dimensions.

Keywords Cortical columns · Integrate-and-fire neurons · Temporal code · Gamma oscillations

Introduction

The synchronization of neurons was proposed as a coding dimension for binding related features (Milner 1974; von der Malsburg 1981; Singer and Gray 1995). One requirement of this hypothesis is that neuronal assemblies are able to modulate their level of synchrony without affecting their firing rate (Singer 1999). A number of studies did not report systematic changes in firing rates while the synchronization pattern within an area was modulated (König et al. 1995; Riehle et al. 1997; Maldonado et al. 2000; Steinmetz et al. 2000; Fries et al. 2001a; Grammont and Riehle 2003). In simulations of neuronal networks, the emergence of synchrony has been investigated (Traub et al. 1996; Wang and Buzsaki 1996; Golomb & Hansel, 2000; Hansel & Mato, 2003 Tiesinga and Sejnowski 2004; Pfeuty et al., 2005) and multiple and complex parameters regimes were characterized. Despite this accumulation of findings, it is still unclear what physiological mechanism the cortex uses.

Synchronization of action potentials can emerge from network dynamics (Jefferys et al. 1996; Ritz and Sejnowski 1997; Sturm and König 2001). For example, oscillatory network activity is often associated with precise timing of spikes (Munk et al. 1996; Herculano-Houzel et al. 1999;

Electronic supplementary material The online version of this article (doi: 10.1007/s11571-007-9017-x) contains supplementary material, which is available to authorized users.

J. Heinzle
Institute of Neuroinformatics, University & ETH Zürich, Winterthurerstrasse 190, 8057 Zürich, Switzerland
e-mail: jakob@ini.phys.ethz.ch

P. König
Institut für Kognitionswissenschaft, University Osnabrück, Albrechtstr. 28, 49069 Osnabrück, Germany
e-mail: pkoenig@uos.de

R. F. Salazar (✉)
Center for Computational Biology, Montana State University, Lewis Hall #1, Bozeman, MT 59717, USA
e-mail: rsalazar@nervana.montana.edu

Fries et al. 2001b), and consequently, is believed to play a role in the synchronized discharge of widely distributed neurons (Gray et al. 1989; König and Schillen 1991; Wang and Buzsaki 1996; Maldonado et al. 2000). Such synchronized activity was shown to occur within as well as between areas (for a review see Engel et al. 2001) and was suggested to operate through intra-areal long range connections (König et al. 1995; Bush and Sejnowski 1996). Importantly, anatomical studies showed that these long-range connections do not solely target excitatory neurons but inhibitory interneurons as well (for a review see Douglas and Martin 2004). Not only was inhibitory activity shown to induce local oscillations (Traub et al. 1996; Wang and Buzsaki 1996; Tiesinga and Sejnowski 2004), but in conjunction with excitatory connections, it is necessary to induce synchronous oscillations between remote neuronal populations (Bush and Douglas 1991; Bush and Sejnowski 1996). Altogether, cortical long-range connections, targeting both excitatory and inhibitory neurons, may play an important role in synchronizing distant groups of neurons.

In the present study, we investigate the relationship between the firing rate and the synchronization of spikes in a simulated network of integrate-and-fire neurons. We investigate whether changes in synaptic weights are sufficient to modulate the synchrony between distant neurons and to keep their firing rates constant. We use a simplified architecture, where a cortical column is composed of one group of excitatory neurons and one group of inhibitory neurons. Connections within and between these groups of neurons take into account transmission delays. The two columns are interconnected by excitatory connections targeting excitatory (E → E) and inhibitory neurons (E → I). Each neuron receives uncorrelated external input consisting of Poisson spike trains. We investigate the oscillatory behavior, the synchrony and the firing rate of the network while varying the strength of the external input and the weights of the E → E and the E → I synapses. We find that a specific balanced modification of long-range synapses onto excitatory and inhibitory neurons modulates the synchronization and oscillatory structure of spikes without affecting their firing rate.

Material and Method

Network architecture

We used a network of integrate-and-fire (IF) neurons to model two cortical columns. Each column consisted of 2000 excitatory (E) and 500 inhibitory (I) neurons. The neurons were randomly connected with a probability of 10%. Thus, within a column there were 400000 excitatory-to-excitatory connections (weight w_{EE}), 100000 excitatory-to-inhibitory connections (w_{IE}), 100000 inhibitory-to-excitatory connections (w_{EI}) and 25000 inhibitory-to-inhibitory connections (w_{II}). The inter-column connectivity was ten times sparser (1%) and consisted of excitatory projections only. Long-range connections of one column consisted of 50000 synapses: 40000 on excitatory neurons (E → E, weight W_{EE}) and 10000 on inhibitory neurons (E → I, W_{IE}). This general organization matches well-based principles of cortical circuitry. The bulk of synaptic connections is local (~90%; Knoblauch et al 2006) and involves both inhibitory and excitatory neurons. The two columns reflect patches of similar neurons, which are connected by long-range axons targeting both excitatory and inhibitory neurons (for review see Douglas and Martin 2004). Synaptic delays were chosen as 0.5 ± 0.2 ms for the local connections and 1.5 ± 0.5 ms for the long range connections. Delays were uniformly distributed within the given range. With an assumed axonal transmission velocity of around 1 mm/ms (Longstaff 2000), this leads to a distance of more than 1 mm between the two columns. A schematic drawing of the network is shown in Figure 1.

We also simulated different sizes of the network by varying the number of excitatory neurons per column from 200 to a maximum of 12800 neurons. The sizes of all other populations were changed proportionally.

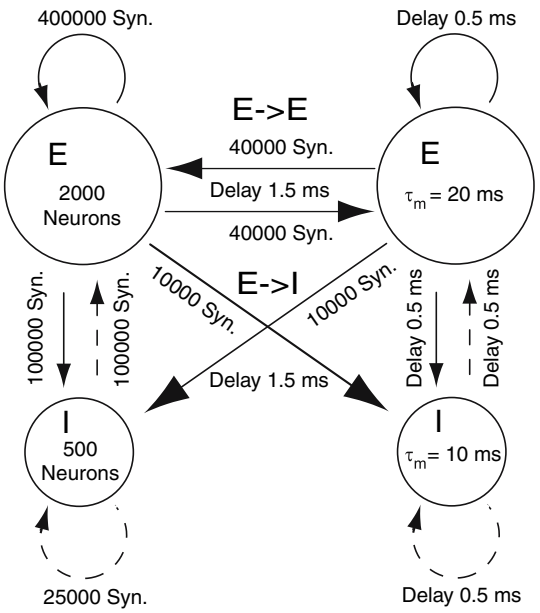

Fig. 1 Schematic drawing of the network structure. Each column contained excitatory (E) and inhibitory (I) conductance-based integrate-and-fire neurons. Parameters for the two types of neurons are given in Table 1. Each neuron received ten uncorrelated external inputs consisting of Poisson spike trains having an exponential distribution of their inter-spike intervals. E → E: long-range connections between excitatory neurons, E → I: long-range connections between excitatory and inhibitory neurons

Neuron model

Conductance based IF neurons were used as the neuron model (for example see Tuckwell, 1988). All neurons, either excitatory or inhibitory, had the same general dynamics given by

$$\tau_m \frac{dV_m}{dt} = (V_0 - V_m) + G_E(V_E - V_m) + G_I(V_I - V_m) + G_{ext}(V_E - V_m) \quad (1)$$

where V_m was the membrane potential of the cell, τ_m was the membrane time constant and V_0 was the resting potential. The excitatory (V_E) and inhibitory (V_I) reversal potentials were the same for both types of neurons. If the membrane voltage crossed a threshold V_t a spike was emitted and the potential was reset to V_r. For the values of the parameters see Table 1.

The synaptic conductances G_E, G_I, and G_{ext} were enhanced by each incoming spike by a weight w and decayed exponentially with time constants $\tau_E = \tau_{ext} = 2$ ms and $\tau_I = 5$ ms:

$$\frac{dG_{E,I}}{dt} = -\frac{G_{E,I}}{\tau_{E,I}} \quad (2)$$

and

$$G_{E,I} \rightarrow G_{E,I} + w \quad (3)$$

for each incoming spike.

The size of single weights depended on the connection. Note, that $G_{E,I}$ in Eq. 1 had no units since the whole equation was multiplied by the leak conductance of excitatory ($g_{leak,E} = 25$ nS) or inhibitory ($g_{leak,I} = 20$ nS) neurons, respectively. We report all weights in Nano Siemens (nS) by multiplying the unitless $G_{E,I}$ in our simulations by the corresponding leak conductances.

Each neuron received an external input composed of 10 Poisson spike trains, each of them having a mean frequency ν_{input}. ν_{input} ranged from 150 to 450 Hz and induced firing rates between 0 and 100 Hz in the excitatory neurons. Each input spike train was computed independently to avoid correlations between them. Hence, this input corresponded to a single poisson spike train of 1,500–4,500 Hz. The synaptic weights of the external inputs were $w_{E,ext} = 2.75$ nS and $w_{I,ext} = 1.8$ nS for the excitatory and the inhibitory neurons respectively. Note that, in the following, we refer to the weight of intra-column and inter-column connections as w and W, respectively.

Synchrony measurement

We assessed intra- and inter-column spike synchronization by computing the respective auto- and cross-correlograms of the excitatory population. The population activity consisted in summing the activity of all the neurons within a column (1 ms bins). The summed spike trains were mean-removed and conventional auto- and cross-correlations were calculated from those normalized spike trains (a normalization by the squared root of the product of the standard deviations of the two random variables results in values of 1.0 for a perfect positive correlation). The first 200 ms of each simulation were not considered for the analysis to avoid synchronous events that were related to the onset of activity at the beginning of each simulation. In cross-correlograms, central peaks were often observed with phases ranging from zero to two milliseconds lags whereas the period of one oscillation could range from 12 to 16 ms. We defined the central peak of the cross-correlograms as the maximum within a window of –2 ms to +2 ms time lag. Instead of choosing this maximal value as a synchrony measure, we preferred to have a measure that can be similarly applied to cross- and auto-correlograms. Therefore, the synchrony was defined as the average of the two bins adjacent to the central peaks. Other synchrony measures (Abeles 1982; Palm et al. 1988) were tested and the analyses yielded qualitatively similar results. The frequency range and power of the synchronous oscillations was assessed from these correlograms using Fourier analysis.

The goal of the study was to vary the strength of the long-range connections and compare its impact on the firing rate, synchrony and synchronous oscillatory activity of the network. For this purpose, we calculated the modulation ratio for each measure as follows:

Table 1 Parameters of the neuron model

	V_t (mV)	V_r (mV)	τ_m (ms)	V_0 (mV)	τ_r (ms)	V_E (mV)	V_I (mV)
E	–52	–59	20	–74	2	0	–80
I	–52	–59	10	–72	1	0	–80

We used the following neuron parameters: threshold potential V_t; reset potential V_r; membrane time constant τ_m; resting potential V_0; refractory time, τ_r. The excitatory (V_E) and inhibitory reversal potentials (V_I) were the same for both types of neurons. Parameters were taken from Wang (2000) and fit the single cell frequency and current relationship reported in McCormick et al. (1985)

$$r_X = \left(\max_W(X_W) - \min_W(X_W)\right) \Big/ \left(\left|\max_W(X_W)\right| + \left|\min_W(X_W)\right|\right) \quad (4)$$

where X was either the firing frequency of the network, the synchrony or the average power of the synchronous oscillations between 0 and 125 Hz for various external input strengths. The maximum and the minimum of X were taken over all values of the weights W_{IE} and W_{EE} that conserved a fixed ratio (see below for details). The absolute values in the denominator ensured that negative synchrony values did not lead to values of $r_X > 1$.

All simulations were run in NEURON (Hines and Carnevale 1997) and all subsequent analyses were performed in MatLab (Mathworks). Iteration steps of the numerical simulation were set to 0.1 ms.

Results

We first simulated a single column. As an initial level of intra-column synchrony is necessary to maintain the modulated parameters within a realistic range (see below for details), we used recurrent inhibition (Brunel and Wang 2003) to set the population synchrony around 0.5. Then, the two columns were simulated interconnected with long-range connections, both excitatory to excitatory neurons (E → E) and excitatory to inhibitory neurons (E → I), for a time period of 2 s. The external input strength and the weight of E → E (W_{EE}) and E → I (W_{IE}) synapses were varied independently. Finally, we performed 70 additional simulations (with 7 × 10 variation of the external input and the long-range synaptic weights with W_{IE} equals 1.6-fold W_{EE}) for input strengths varying from 150 to 450 Hz. To investigate the dynamics of single pairs and small populations of neurons we also ran long simulations of 30 s.

Spiking and synchrony of a single column

We first simulated a single column with an external input of 300 Hz (v_{input}) and adjusted excitatory and inhibitory synaptic weights to set the intra-column synchrony around 0.5. The synaptic weights within the columns were set to the following: w_{EE} = 0.25 nS, w_{IE} = 0.4 nS, w_{EI} = 0.5 nS and w_{II} = 0.4 nS. These values closely approximate the characteristic excitatory-inhibitory balanced inputs into cortical neurons (Destexhe et al. 2003). Figure 2A shows membrane voltage traces and raster plots for excitatory and inhibitory neurons in a single column. Synchronous oscillations are noticeable in the raster plots but this oscillatory activity is not obvious for single neurons. The distribution of firing rates and coefficients of variation (CV) for single neurons are shown in Fig. 2B and C, respectively. They show that the firing rate of single neurons expands from 0 to 200 Hz (Fig. 2B), and that the variability of the spike trains (Fig. 2C) resembles the variability observed in biological neurons (Softky and Koch 1993).

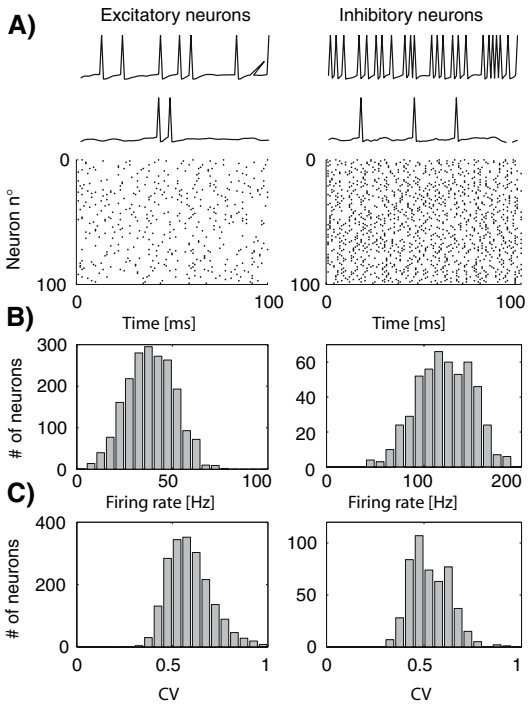

Fig. 2 Firing properties of a single column. Properties of single cell activity are shown for the excitatory (left) and inhibitory (right) populations within a column. External stimulus strength was 300 Hz. (**A**) Sample traces of a highly active and a less active neuron are shown above a raster plot of the spikes from the whole population. (**B**) Spike rastergrams for 100 sample neurons of one excitatory and inhibitory population. The mean and median firing rates are 38 Hz and 38 Hz (25th and 75th percentiles are 30 and 48 Hz, respectively) for excitatory neurons and 121 Hz and 120 Hz (25th and 75th percentiles are 100 and 142 Hz respectively) for inhibitory neurons. (**C**) Distribution of the coefficients of variation for single neurons. The mean and median are 0.59 and 0.58 (25th and 75th percentiles are 0.51 and 0.66 respectively) for excitatory neurons and 0.53 and 0.52 (25th and 75th percentiles are 0.45 and 0.61 respectively) for inhibitory neurons

Rate, synchrony and oscillations with long-range connections

Once the intra-column parameters were set, we simulated two columns of neurons and varied the weights of long-range projections. We investigated the influence of inter-column synaptic weights and the external input strength on the firing rate, synchrony and the synchronous oscillations of the network. W_{EE} and W_{IE} were varied from 0 to 1.8 nS and from 0 to 2.88 nS, respectively. These variations were applied for all the neurons simultaneously and performed independently from each other at two different input strengths, 300 and 450 Hz.

In the right panels of Fig. 3, we observe that the firing rate is proportional to the input strength and to W_{EE} and inversely proportional to W_{IE}. As changes in W_{EE} and W_{IE} have opposite effects, it is intuitive that an appropriate tuning of these two parameters should maintain the firing rate of the excitatory neuron constant. We find that a value of 1.6 for W_{EE}/W_{IE} keeps the firing rate constant. The fact that the relationship between W_{EE} and W_{IE} is linear is explained in the supplementary material. Less obvious is to know whether the balanced change in the weights can modulate the inter-column synchrony and how the strength of the oscillations and the intra-column synchrony are affected.

The intra-column synchrony follows a pattern similar to the firing rate when the external input is 300 Hz. It is proportional to W_{EE} and inversely proportional to W_{IE} (Fig. 3A; left panel). This induces that the values on the diagonal of the horizontal axes (green dashed lines) are maintained constant. In contrast, the inter-column synchrony is modulated along this diagonal and increases with increasing W_{EE} and W_{IE} (Fig. 3A; middle panel). When the external input is 450 Hz, we observe a different behavior in the intra-column synchrony. Only a covariation of the inter-column weights affects the level of synchrony (Fig. 3B; middle panel). One explanation is that both excitatory and inhibitory neurons need to be sufficiently

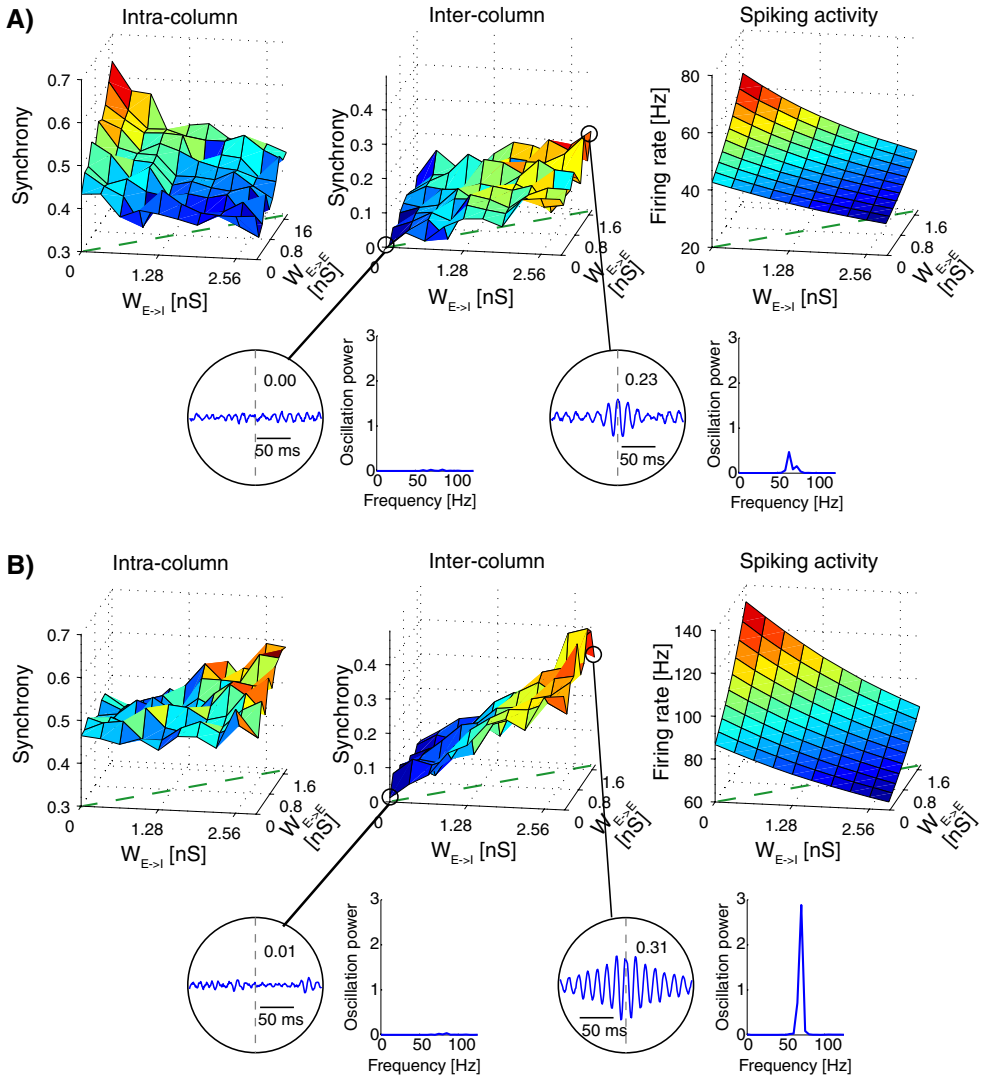

Fig. 3 Behavior of the network under two different external input strengths. The intra- and inter-column synchrony and the spiking activity are shown as a function of the weights W_{EE} and $W_{I.E}$ and for external input frequencies of 300 Hz (**A**) and 450 Hz (**B**). In the lower insets, examples of cross-correlograms are plotted. The upper values in these insets correspond to the level of synchrony. On the right side of these insets, the power spectra of the cross-correlograms are shown. Note that the relationship between the long-range synaptic weights (W_{EE} and $W_{I.E}$) and the different measures change with different external inputs. Nevertheless, along the diagonal (green dashed lines) where W_{IE}/W_{EE} equals 1.6 this relationship is conserved: the spiking activity remains constant while the inter-column synchrony is increased from around zero to above 0.2 (**A**) and 0.4 (**B**)

driven by the external input to work in synergy and to modulate intra-column synchrony. Otherwise, W_{EE} facilitates the intra-column synchrony via mutual excitation and W_{IE} affects it in an opposite direction probably due to a detrimental increase in inhibition (Bush and Sejnowski 1996). Despite these differences, one interesting characteristic is maintained in the two external input regimes. Maintaining a specific fixed ratio between W_{EE} and W_{IE} keeps the spiking rate constant while the inter-column synchrony is modulated.

To visualize this effect better, we plot in Fig. 4A the values of the firing rate (upper panel), synchrony (second and third panels) and the average (from 0 to 125 Hz) power of the oscillations (forth and fifth panels) along this diagonal. The different colors correspond to different external input strengths, which shows that the external input controls the firing rate of the network as well as the peak of the power spectra of the synchronous oscillations (Fig. 4B).

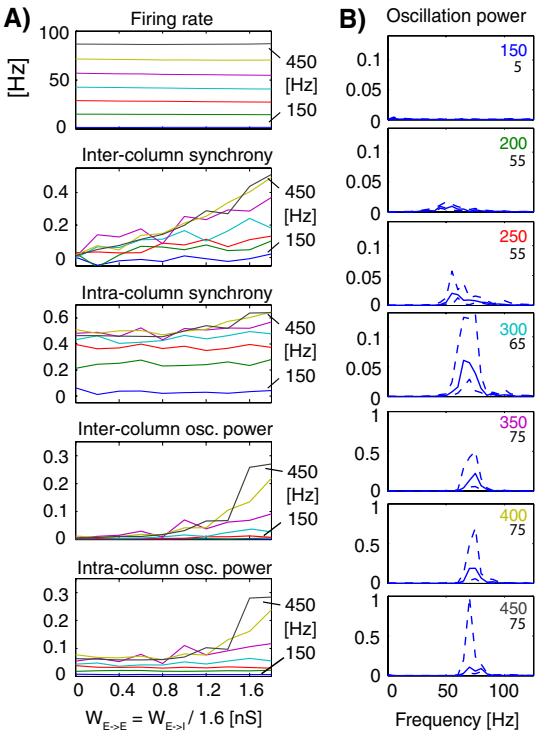

Fig. 4 Population responses to various input strengths with a fixed W_{IE}/W_{EE} ratio. In (**A**), we plotted the spiking activity (upper panel), the inter- and intra-column synchrony (second and third panel) and the inter- and intra-column oscillation power (forth and fifth panel). Note that the different colors correspond to different external input strengths ranging from 150 to 450 Hz. The modulation ratios of all the curves are given in Table 2. In (**B**), the distribution of the power spectra for all W_{EE} and W_{IE} are presented. The solid lines correspond to the medians and the upper and lower dashed lines are the 75th and 25th percentiles. The colored numbers refer to the different external input frequencies and the black number is the frequency at the maximum power

We observe again that the firing rate of the two columns is not affected by a balanced change in W_{EE} and W_{IE} (Fig. 4A). It is important to emphasize that not only is the excitatory rate maintained constant but the overall firing rate as well (Table 2). Certainly, the inhibitory rates are slightly modulated. However, their modulation is much weaker roughly seven to ten times less than the modulation of the inter-column synchrony (Table 2). This means that the maintenance of the firing rate is fulfilled by the whole network.

In contrast, the synchrony and the power of the oscillations are considerably modulated by the synaptic weights of the long-range connections (Table 2), even when longer inter-column delays, up to 5 ms, were used. In these simulations, the synchronization level was lower and occurred with larger phase lags (data not shown). Nevertheless, the modulation ratios of rate and synchrony were comparable to the ones obtained with the shorter delay (Table 3). The modulation ratio of the synchrony was at least ten times the modulation ratio of the firing rate for all settings of the input.

However, an initial level of intra-column synchrony is still necessary for the modulation to take place. For example, when the intra-column synchrony is low (blue and green line), the modulation of the inter-column synchrony is poor (Fig. 4A). The cause of this effect is not the level of activity per se but the level of intra-column synchrony because when we used a weight-configuration that led to high firing rates but low intra-column synchrony (~0.2), only nonrealistic enormous increases in W_{EE} and W_{IE} could modulate the inter-column synchrony (data not shown). These results suggest that an initial level of synchronous oscillations is necessary within each column to enable the inter-column connections to have an effect. To further characterize this effect, we measured the phase lag between the two columns at different weight configurations. We notice that the phase at the frequency of oscillation, the gamma range (Fig. 4B), approaches to zero as the weights are increased (Fig. 5). Thus, the role of the long-range connections is to reduce the phase lag between the existing intra-column synchronous oscillations, and thereby, to synchronize the two columns.

Size effects

To evaluate if the number of neurons in our network impedes on the validity of our finding, we investigated how the modulation ratios varied when the number of excitatory neurons per column is changed to 200, 400, 800, 1,600, 3,200, 6,400, and 12,800. The number of inhibitory neurons was changed proportionally. The connectivity was established in two different manners: (1) We kept the connectivity at 10% and therefore the number of synapses

Table 2 Ratios of modulation in population responses

	External input strength (Hz)						
	150	200	250	300	350	400	450
Excitatory rate	0.03	0.02	0.03	0.02	0.02	0.01	0.00
Inhibitory rate	0.10	0.10	0.09	0.08	0.08	0.08	0.08
Firing rate	0.05	0.03	0.02	0.03	0.03	0.03	0.04
Inter-column synchrony	1.00	1.00	0.64	1.00	0.98	0.94	0.95
Intra-column synchrony	0.66	0.14	0.07	0.10	0.14	0.16	0.17
Inter-column oscillations	0.40	0.51	0.65	0.77	0.91	0.94	0.97
Intra-column oscillations	0.12	0.11	0.14	0.28	0.43	0.60	0.66

Table 3 Ratios of modulation at different inter-column delays

	External input strength (Hz) Delay			
	300 3 ms	300 5 ms	450 3 ms	450 5 ms
Excitatory rate	0.02	0.00	0.02	0.02
Inhibitory rate	0.08	0.08	0.08	0.09
Firing rate	0.02	0.04	0.02	0.05
Inter-column synchrony	1.00	0.93	0.86	0.89
Intra-column synchrony	0.07	0.12	0.06	0.29
Inter-column oscillations	0.59	0.88	0.80	0.99
Intra-column oscillations	0.11	0.48	0.23	0.92

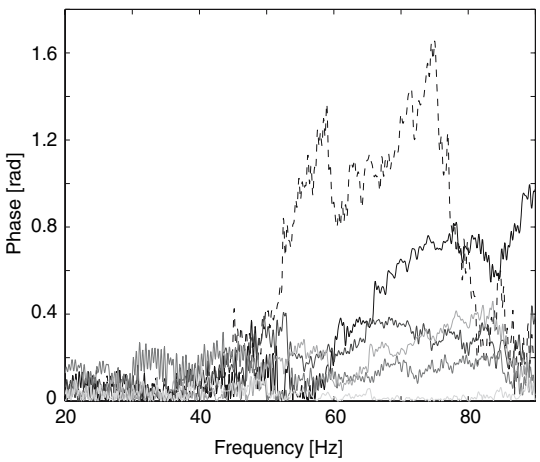

Fig. 5 Phase lag between the population activity of the two columns as a function of frequency. The different curves represent different inter-column weight configuration ($W_{IE} = 1.6\ W_{EE}$) with W_{EE} ranging from zero (dashed line) to 1.0 nS (black to light gray for increasing weights). The simulations were run at 300 Hz for the external input strength. Values for W_{EE} above 1.0 nS are not shown for clarity reasons; they roughly follow the light gray curve and are always below 0.2 radians. The frequency range was chosen between 20 and 90 Hz because the values are either around zero (<20 Hz) or are not reliable due to low coherence values (>90 Hz). A multi-taper method (40 tapers) was used to estimate the phase over the 2 s period of the simulation

was proportional to the number of neurons to the square. To keep the average input to each neuron constant, the weights were scaled inversely to the number of neurons. In this case, we stopped the simulations at 6,400 neurons. (2) The number of synapses was proportional to the number of neurons in the network, and the weights were kept constant. Each neuron received on average 40 intra-columnar excitatory inputs. All other connections scaled proportionally.

In both cases, we find that the modulation of synchrony remains constant and elevated whereas the modulation ratios of the firing rates are lower (Fig. 6A, C, E). Therefore, our finding that the synchrony can be modulated without changes in firing rates is also valid for smaller and larger networks.

Dynamic of small groups of neurons

So far, we reported the results at the population level only. However, the randomness of the connections and the various firing regimes observed in single neurons (Fig. 2) suggest considerable variability at the level of individual pairs. Therefore, we investigated the relationship between firing rate and synchrony in single pairs of neurons and in small groups of neurons. For this purpose, we increased the duration of the simulations to 30 s and only investigated

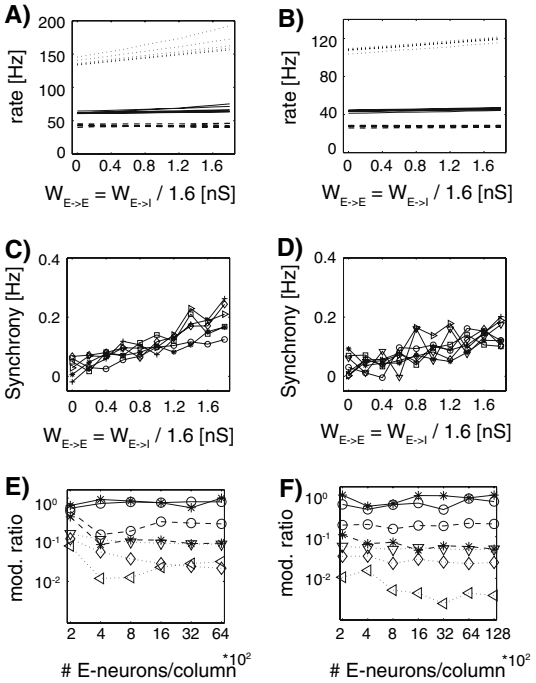

Fig. 6 Effect of network size. In (**A**) and (**B**) the firing rates are shown as a function of W_{EE}; $W_{IE} = 1.6\ W_{EE}$. Solid lines: all neurons, dashed lines: excitatory neurons, dotted lines: inhibitory neurons. Different curves correspond to different network sizes. (**C**) and (**D**) show the inter-column synchrony as a function of W_{EE}. Different markers indicate different network sizes: 200 excitatory neurons per column (circles), 400 (stars), 800 (squares), 1,600 (triangles pointing to the right) 3,200 (diamonds), 6,400 (crosses), and 12,800 (triangles pointing down). In (**E**) and (**F**) the log–log plots of the modulation ratios as function of network size are shown: inter-column synchrony (solid, stars), inter-column oscillations (solid, circles), intra-column synchrony (dashed, stars), intra-column oscillations (dashed, circles), rate of all neurons (dotted, diamonds), rate of excitatory neurons (dotted, triangles left) and rate of inhibitory neurons (dotted, triangles down). **A**, **C**, and **E** correspond to case 1 (10% connectivity in all networks); **B**, **D**, and **F** correspond to case 2 (number of synapses proportional to the number of neurons)

cases where the equilibrium ratio of the weights ($W_{IE}/W_{EE} = 1.6$) was satisfied. First, we looked at the distribution of firing rates of individual cells. Then, we randomly selected 100 neurons in each column and computed the synchrony between all possible pairs of neurons between these two groups. This was done irrespective of the connectivity of the neurons, thus mimicking an electrophysiological experiment. The distribution of the rates and ''single-cell'' synchrony are shown in Fig. 7A and B. A first observation is that, in general, the level of synchrony between single neurons is small compared to the synchrony measured at the whole population level (Fig. 4A); a fact previously observed in a comparable neural network (Brunel and Wang 2003) and in electrophysiological recordings (Bedenbaugh and Gerstein 1997; Gerstein 2000). Second, the firing rate and the synchrony between

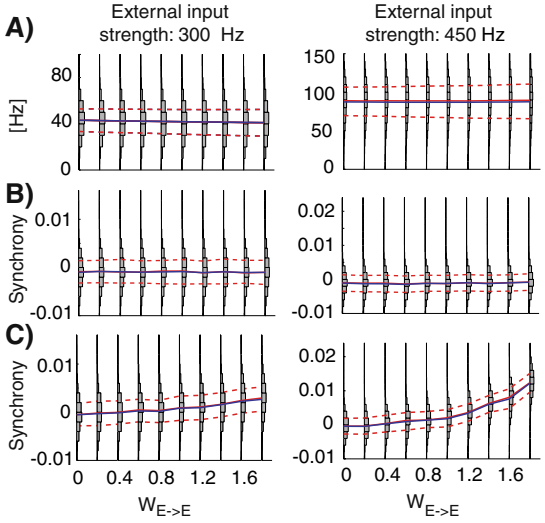

Fig. 7 Distribution of firing rates (single cells) and synchrony (single cells and groups of cells) for various weights configurations ($W_{IE}/W_{EE} = 1.6$). Each panel represents the normalized distributions at different weight configurations. The distributions were obtained from the whole period of 30 s for 300 Hz (left panel) and 450 Hz (right panel) inputs strength. The averaged rate data is presented for the firing rate of all excitatory cells in the two columns (**A**, $n = 4{,}000$). The inter-column synchrony of single cells was calculated for all possible pairs of 100 randomly selected neurons of each column (**B**, $n = 10{,}000$) and the inter-column group synchrony (**C**) was calculated for 1,000 pairs of randomly selected groups of neurons ($n = 20$). The lines in the graphs summarize the histograms, showing the mean (*blue resp. black in the printed version*), the median (*red resp. gray in the printed version*), as well as the 25th and 75th percentile (black dashes) of the distribution for the ten different weights

single cells are not modulated by changes in synaptic weights (Fig. 7A and B). On the other hand, when we did 1,000 measurements between two randomly selected groups of 20 neurons in each column, we could detect a modulation in the average synchrony and its distribution (Fig. 7C). Interestingly, the distribution is unimodal, which suggests that the strength of the observed synchrony at the population level is mainly attributable to a summation effect and not to specific subpopulations of neurons.

Discussion

In a cortical network, the efficacy of excitatory long-range connections modulates inter-column synchrony, synchronous oscillations and the firing rate of neurons. However, in excitatory neurons, it is possible to modulate the degree of synchronization independently from effects on the spike rate by modifying the synaptic weights of postsynaptic excitatory (W_{EE}) and inhibitory (W_{IE}) neurons in a linear manner.

The firing rate of the excitatory population is kept constant if the long-range projections drive the excitatory

neurons proportionally to the inhibitory neurons. In our study, the ratio was 1.6 (W_{IE}/W_{EE}). However, this exact value depends of course on the parameters of the simulation such as the number of synapses, the relative firing rates of excitatory and inhibitory neurons and the time constants of different synaptic events. For example, we found this ratio to be 1.0 in a homogenous network of 100 identical excitatory and 100 inhibitory neurons per column (Salazar et al. 2004a). More importantly, this ratio reflects the linear relationship between W_{IE} and W_{EE} as a result of the nearly linear f–I curves of the IF-neurons. Any other monotonically increasing f–I curve should lead to a solution of balanced W_{IE} and W_{EE}, which, however, is not necessarily linear. On the other hand, to know whether changes in the inter-column weights modulate the inter-column synchrony accordingly cannot be predicted without large-scale simulations. Therefore, a detailed description of the network behavior is necessary to acquire a mechanistic understanding of the phenomenon.

In this study, we demonstrate that neuronal networks can modulate their inter-column synchronous activity by linearly altering both W_{EE} and W_{IE}. To maintain this modulation within a reasonable parameter range, we introduced a certain amount of synchronous activity within each column using recurrent inhibition. This mechanism was shown to synchronize the populations activity of integrate-and-fire neurons in the gamma frequency range (Brunel and Wang 2003); a range that we also observed in the oscillations within, as well as between, columns and that was proposed to play an important role in intra-areal synchronization of activity (for reviews see von Stein and Sarnthein 2000; Engel et al. 2001). The synchronization of distant populations of neurons raises a couple of issues, one being the transmission delay. If this delay is too long, the synchronization breaks down (Bush and Sejnowski 1996). We find that the modulation ratios of rate and synchrony were comparable if the inter-column synaptic delay is increased to 5 ms. Furthermore, despite the fact that model networks composed of other kinds of neurons may show more realistic behavior with respect to synchrony and fluctuations (Fourcaud-Trocmé et al. 2003), our main findings are still valid even when we use quadratic integrate-and-fire neurons (see supplementary material). Finally, a modulation of the inter-column synchronization independently from the firing rate is still achieved in various networks size despite the relationship between the synchrony and the number of neurons (Brunel and Hakim 1999; Hansel and Mato 2003). Altogether, our simulations demonstrate that the role of long-range connections is to synchronize the gamma oscillations occurring within each column and to reduce their phase lag.

Interestingly, this effect is only observed at the population and subpopulation level. The synchrony between single neurons is virtually zero and is not modulated by changes in synaptic weights. One explanation is that single neurons do not participate in each cycle of the oscillating network or if they do, that they are not precisely locked to the oscillation (>2 ms). Thus, when pair-wise correlations are calculated, they are weak. A comparable phenomenon was described in another theoretical study (Brunel and Wang 2003) where the behavior of single neurons did not precisely follow the oscillations of the population. Effectively, activity of single neurons can often follow loosely the dominant oscillations, as observed in electrophysiological recordings. For example, in the hippocampus, single neurons fire more or less precisely during theta oscillations but they do not participate in every cycle (Buzsaki and Eidelberg 1983; Buzsaki et al. 1983; Kamondi et al. 1998; Csicsvari et al. 1999). Thus, certain properties of neuronal ensembles are difficult to derive from the activity of few single neurons, which raises important restrictions to the experimental investigation of population coding (Deadwyler and Hampson 1997). Our results predict that a modulation of synchronization attributable to learning should be detectable in population measures such as local field potentials or multi-unit recordings but unlikely in pairs of single cells.

A last point that deserves discussion is whether it is realistic to have synaptic plasticity in cortical post-synaptic inhibitory neurons. Most of the previous studies have focused exclusively on the plasticity of W_{EE} (for a review see Abbott and Nelson 2000). Certainly, it is the most commonly studied type of plasticity. However, W_{IE} was described in the hippocampus (Perez et al. 2001; Lapointe et al. 2004) and in the cerebellum (Kano et al. 1992) as well. We propose that a mechanism that changes the weights of long range EE and EI connections in a similar way could induce a modulation of synchrony without consistent changes in the firing rate. Several electrophysiological recordings of single cells and local field potentials (König et al. 1995; Vaadia et al. 1995; Riehle et al. 1997; Fries et al. 2001a; Grammont and Riehle 2003; Salazar et al. 2004a) reported differences in neuronal synchronizations, and not in firing rates, between behavioral/stimulus conditions. Tiesinga and Sejnowski (2004) proposed a mechanism in which a rapid activation of a few selected interneurons produces such an effect. One difference between their proposal and ours is their inclusion of ''top-down'' information, that is, which group of interneurons should be selected. This requirement is well suited to, and inspired from, attentional processes. On the other hand, our proposal does not require such information and works well in a simple ''bottom-up'' processing. Therefore, these two mechanisms may well explain different processes and may not be mutually exclusive. Finally, our model is based on two biological plausible assumptions: the plasticity of W_{IE}

in the cortex and the ability to modify these synapses proportionally to W_{EE}. The end result is simply to balance neuronal activity using homeostatic plasticity; a basic principle repetitively observed in various systems (for a review see Turrigiano and Nelson 2004). However, the implementation of such a mechanism in neuronal networks is still an open question.

In conclusion, with simple changes in synaptic weights, the degree of synchronized activity can be modulated independently from the firing rate. In the last decade, various reports have supported the notion that mature sensory areas can modify their synapses (Artola and Singer 1987; Schuett et al. 2001; Yao and Dan 2001; Fu et al. 2002) according to behavioral requirements (Recanzone et al. 1992, 1993; Bao et al. 2001, 2004). Such synaptic changes may enable the modulation of neuronal temporal interactions (Crist et al. 2001; Schwartz et al. 2002; Salazar et al. 2004b) without potential interferences with the mean level of activity (Schoups et al. 2001; Ghose et al. 2002; Salazar et al. 2004b). This facilitates the use of synchronous activity and the firing rate of neurons to cooperatively process different types of information (Neven and Aertsen 1992; Salinas and Sejnowski 2001). Therefore, it is tempting to speculate that cortical networks use two coding schemes, but more importantly, that one can remain stable while the other is plastic and sensitive to learning. Such a mechanism can be a solution to the *stability-plasticity dilemma* confronted by sensory systems.

Acknowledgements This work was funded by the Swiss National Science Foundation (Grant Nr: 31-65415.01). We thank Kevan AC Martin, Charles M Gray, Stefano Fusi and Shih-Cheng Yen for their careful reading and critical comments on previous versions of the manuscript.

References

Abbott LF, Nelson SB (2000) Synaptic plasticity: taming the beast. Nat Neurosci 3:1178–1183

Abeles M (1982) Local cortical circuits. An electrophysiological study. Springer, Berlin

Artola A, Singer W (1987) Long-term potentiation and NMDA receptors in rat visual cortex. Nature 330:649–652

Bao S, Chan VT, Merzenich MM (2001) Cortical remodelling induced by activity of ventral tegmental dopamine neurons. Nature 412:79–83

Bao S, Chang EF, Woods J, Merzenich MM (2004) Temporal plasticity in the primary auditory cortex induced by operant perceptual learning. Nat Neurosci 7:974–981

Bedenbaugh P, Gerstein GL (1997). Multiunit normalized cross correlation differs from the average single-unit normalized correlation. Neural Comput 9(6):1265–1275

Brunel N, Hakim V (1999) Fast global oscillations in networks of integrate-and-fire neurons with low firing rates. Neural Comput 11(7):1621–1671

Brunel N, Wang XJ (2003) What determines the frequency of fast network oscillations with irregular neural discharges? I. Synaptic dynamics and excitation-inhibition balance. J Neurophysiol 90:415–430

Bush PC, Douglas RJ (1991) Synchronization of bursting action potential discharge in a model network of neocortical neurons. Neural Comp 3:19–30

Bush PC, Sejnowski TJ (1996) Inhibition synchronizes sparsely connected cortical neurons within and between columns in realistic network models. J Comp Neurosci 3:91–110

Buzsaki G, Eidelberg E (1983) Phase relations of hippocampal projection cells and interneurons to theta activity in the anesthetized rat. Brain Res 266:334–339

Buzsaki G, Leung LW, Vanderwolf CH (1983) Cellular bases of hippocampal EEG in the behaving rat. Brain Res 287:139–171

Crist RE, Li W, Gilbert CD (2001) Learning to see: experience and attention in primary visual cortex. Nat Neurosci 4:519–525

Csicsvari J, Hirase H, Czurko A, Mamiya A, Buzsaki G (1999) Oscillatory coupling of hippocampal pyramidal cells and interneurons in the behaving Rat. J Neurosci 19:274–287

Deadwyler SA, Hampson RE (1997) The significance of neural ensemble codes during behavior and cognition. Annu Rev Neurosci 20:217–244

Destexhe A, Rudolph M, Pare D (2003) The high-conductance state of neocortical neurons in vivo. Nat Rev Neurosci 4:739–751

Douglas RJ, Martin KA (2004) Neuronal circuits of the neocortex. Annu Rev Neurosci 27:419–451

Engel AK, Fries P, Singer W (2001) Dynamic predictions: oscillations and synchrony in top-down processing. Nat Rev Neurosci 10:704–716

Fourcaud-Trocmé N, Hansel D, van Vreeswijk C, Brunel N. (2003) How spike generation mechanisms determine neuronal response to fluctuating inputs. J Neurosci 23(37):11628–11640

Fries P, Reynolds JH, Rorie AE, Desimone R (2001a) Modulation of oscillatory neuronal synchronization by selective visual attention. Science 291:1560–1563

Fries P, Neuenschwander S, Engel AK, Goebel R, Singer W (2001b) Rapid feature selective neuronal synchronization through correlated latency shifting. Nat Neurosci 4:194–200

Fu YX, Djupsund K, Gao H, Hayden B, Shen K, Dan Y (2002) Temporal specificity in the cortical plasticity of visual space representation. Science 296:1999–2003

Gerstein GL (2000). Cross-correlation measures of unresolved multi-neuron recordings. J Neurosci Methods 100(1–2):41–51

Ghose GM, Yang T, Maunsell JH (2002) Physiological correlates of perceptual learning in monkey V1 and V2. J Neurophysiol 87:1867–1888

Golomb D, Hansel D (2000) The number of synaptic inputs and the synchrony of large, sparse neuronal networks. Neural Comput 12:1095–1139

Grammont F, Riehle A (2003) Spike synchronization and firing rate in a population of motor cortical neurons in relation to movement direction and reaction time. Biol Cybern 88:360–373

Gray CM, König P, Engel AK, Singer W (1989) Oscillatory responses in cat visual cortex exhibit inter-columnar synchronization which reflects global stimulus properties. Nature 338:334–337

Hansel D, Mato G (2003) Asynchronous states and the emergence of synchrony in large networks of interacting excitatory and inhibitory neurons. Neural Comput 15:1–56

Herculano-Houzel S, Munk MH, Neuenschwander S, Singer W (1999) Precisely synchronized oscillatory firing patterns require electroencephalographic activation. J Neurosci 19:3992–4010

Hines ML, Carnevale NT (1997) The NEURON simulation environment. Neural Comput 9:1179–1209

Jefferys JG, Traub RD, Whittington MA (1996) Neuronal networks for induced '40 Hz' rhythms. Trends Neurosci 19:202–208

Kamondi A, Acsady L, Wang XJ, Buzsaki G (1998) Theta oscillations in somata and dendrites of hippocampal pyramidal cells in vivo: activity-dependent phase-precession of action potentials. Hippocampus 8:244–261

Kano M, Rexhausen U, Dreessen J, Konnerth A (1992) Synaptic excitation produces a long-lasting rebound potentiation of inhibitory synaptic signals in cerebellar Purkinje cells. Nature 356:601–604

Knoblauch K, Falchier A, Giroud P, Kennedy H (2006) Areas V1, V2, and V4 have fixed numbers of connections from each afferent area. 2006 Abstract Viewer/Itinerary planner: Atlanta: Society for Neuroscience

König P, Schillen TB (1991) Stimulus-dependent assembly formation of oscillatory responses: I. Synchronization. Neural Comput 3:155–166

König P, Engel AK, Singer W (1995) Relation between oscillatory activity and long-range synchronization in cat visual cortex. Proc Natl Acad Sci USA 92:290–294

Lapointe V, Morin F, Ratte S, Croce A, Conquet F, Lacaille JC (2004) Synapse-specific mGluR1-dependent long-term potentiation in interneurones regulates mouse hippocampal inhibition. J Physiol 555:125–135

Longstaff A (2000) Neuroscience. BIOS Scientific Publishers Ltd, Oxford (UK)

Maldonado PE, Friedman-Hill S, Gray CM (2000) Dynamics of striate cortical activity in the alert macaque: II. Fast time scale synchronization. Cereb Cortex 10(11):1117–1131

McCormick DA, Connors BW, Lighthall JW, Prince DA (1985) Comparative electrophysiology of pyramidal and sparsely spiny stellate neurons of the neocortex. J Neurophysiol 54:782–806

Milner PM (1974) A model for visual shape recognition. Psychol Rev 81:521–535

Munk MH, Roelfsema PR, König P, Engel AK, Singer W (1996) Role of reticular activation in the modulation of intracortical synchronization. Science 272:271–274

Neven H, Aertsen A (1992) Rate coherence and event coherence in the visual cortex: a neuronal model of object recognition. Biol Cybern 67:309–322

Palm G, Aertsen AM, Gerstein GL (1988) On the significance of correlations among neuronal spike trains. Biol Cybern 59:1–11

Perez Y, Morin F, Lacaille JC (2001) A hebbian form of long-term potentiation dependent on mGluR1a in hippocampal inhibitory interneurons. Proc Natl Acad Sci USA 98:9401–9406

Pfeuty B, Mato G, Golomb D, Hansel D (2005) The combined effects of inhibitory and electrical synapses in synchrony. Neural Comput 17:633–670

Recanzone GH, Merzenich MM, Jenkins WM, Grajski KA, Dinse HR (1992) Topographic reorganization of the hand representation in cortical area 3b owl monkeys trained in a frequency-discrimination task. J Neurophysiol 67:1031–1056

Recanzone GH, Schreiner CE, Merzenich MM (1993) Plasticity in the frequency representation of primary auditory cortex following discrimination training in adult owl monkeys. J Neurosci 13:87–103

Riehle A, Grun S, Diesmann M, Aertsen A (1997) Spike synchronization and rate modulation differentially involved in motor cortical function. Science 278:1950–1953

Ritz R, Sejnowski TJ (1997) Synchronous oscillatory activity in sensory systems: new vistas on mechanisms. Curr Opin Neurobiol 7:536–546

Salazar RF, König P, Heinzle J (2004a) Synchronization and firing rates as independent coding dimensions. 2004 Abstract Viewer/Itinerary planner. Society for Neuroscience, Washington D.C.

Salazar RF, Kayser C, König P (2004b) Effects of training on neuronal activity and interactions in primary and higher visual cortices in the alert cat. J Neurosci 24:1627–1636

Salinas E, Sejnowski TJ (2001) Correlated neuronal activity and the flow of neural information. Nat Rev Neurosci 2:539–550

Schoups A, Vogels R, Qian N, Orban G (2001) Practising orientation identification improves orientation coding in V1 neurons. Nature 412:549–553

Schuett S, Bonhoeffer T, Hubener M (2001) Pairing-induced changes of orientation maps in cat visual cortex. Neuron 32:325–337

Schwartz S, Maquet P, Frith C (2002) Neural correlates of perceptual learning: a functional MRI study of visual texture discrimination. Proc Natl Acad Sci USA 99:17137–17142

Singer W (1999) Neuronal synchrony: a versatile code for the definition of relations? Neuron 24:49–65, 111–125

Singer W, Gray CM (1995) Visual feature integration and the temporal correlation hypothesis. Annu Rev Neurosci 18:555–586

Softky WR, Koch C (1993) The highly irregular firing of cortical cells is inconsistent with temporal integration of random EPSPs. J Neurosci 13:334–350

Steinmetz PN, Roy A, Fitzgerald PJ, Hsiao SS, Johnson KO, Niebur E (2000) Attention modulates synchronized neuronal firing in primate somatosensory cortex. Nature 404:187–190

Sturm AK, König P (2001) Mechanisms to synchronize neuronal activity. Biol Cybern 84:153–172

Tiesinga PHE, Sejnowski TJ (2004) Rapid modulation of synchrony by competition in cortical interneuron networks. Neural Comput 16:251–275

Traub RD, Whittington MA, Stanford IM, Jefferys JG (1996) A mechanism for generation of long-range synchronous fast oscillations in the cortex. Nature 383:621–624

Tuckwell HC (1988) Introduction to theoretical neurobiology. Cambridge University Press, Cambridge

Turrigiano GG, Nelson SB (2004) Homeostatic plasticity in the developing nervous system. Nat Rev Neurosci 5:97–107

Vaadia E, Haalman I, Abeles M, Bergman H, Prut Y, Slovin H, Aertsen A (1995) Dynamics of neuronal interactions in monkey cortex in relation to behavioural events. Nature 373:515–518

von der Malsburg C (1981) The correlation theory of brain function. Internal report Max-Planck Institute for Biophysical Chemistry, Göttingen, West-Germany

von Stein A, Sarnthein J (2000) Different frequencies for different scales of cortical integration: from local gamma to long range alpha/theta synchronization. Int J Psychophysiol 38(3):301–313

Wang LY (2000) The dynamic range for gain control of NMDA receptor-mediated synaptic transmission at a single synapse. J Neurosci 20:RC115

Wang XJ, Buzsaki G (1996) Gamma oscillation by synaptic inhibition in a hippocampal interneuronal network model. J Neurosci 16:6402–6413

Yao H, Dan Y (2001) Stimulus timing-dependent plasticity in cortical processing of orientation. Neuron 32:315–323